



Get Clarity On Generics

Cost-Effective CT & MRI Contrast Agents

**FRESENIUS
KABI**

[WATCH VIDEO](#)

AJNR

Low-Grade Glioma: Correlation of Short Echo Time ^1H -MR Spectroscopy with ^{23}Na MR Imaging

R. Bartha, J.F. Megyesi and C.J. Watling

AJNR Am J Neuroradiol 2008, 29 (3) 464-470

doi: <https://doi.org/10.3174/ajnr.A0854>

<http://www.ajnr.org/content/29/3/464>

This information is current as of August 29, 2025.

R. Bartha
J.F. Megyesi
C.J. Watling

Low-Grade Glioma: Correlation of Short Echo Time ^1H -MR Spectroscopy with ^{23}Na MR Imaging

BACKGROUND AND PURPOSE: There is considerable variability in the clinical behavior and treatment response of low-grade (WHO grade II) gliomas. The purpose of this work was to characterize the metabolic profile of low-grade gliomas by using short echo time ^1H -MR spectroscopy and to correlate metabolite levels with MR imaging-measured sodium (^{23}Na) signal intensity. Based on previous studies, we hypothesized decreased *N*-acetylaspartate (NAA) and increased myo-inositol (mIns), choline (Cho), glutamate (Glu), and ^{23}Na signal intensity in glioma tissue.

MATERIALS AND METHODS: Institutional ethics committee approval and informed consent were obtained for all of the subjects. Proton (^1H -MR) spectroscopy (TR/TE = 2200/46 ms) and sodium (^{23}Na) MR imaging were performed at 4T in 13 subjects (6 women and 7 men; mean age, 44 years) with suspected low-grade glioma. Absolute metabolite levels were quantified, and relative ^{23}Na levels were measured in low-grade glioma and compared with the contralateral side in the same patients. Two-sided Student *t* tests were used to test for statistical significance.

RESULTS: Significant decreases were observed for NAA ($P < .001$) and Glu ($P = .004$), and increases were observed for mIns ($P = .003$), Cho ($P = .025$), and sodium signal intensity ($P < .001$) in low-grade glioma tissue. Significant correlations ($r^2 > 0.25$) were observed between NAA and Glu ($P < .05$) and between NAA and mIns ($P < .01$). Significant correlations were also observed between ^{23}Na signal intensity and NAA ($P < .01$) and between ^{23}Na signal intensity and Glu ($P < .01$). Ratios of NAA/mIns, NAA/ ^{23}Na , and NAA/Cho were altered in glioma tissue ($P < .001$); however based on the *t* statistic, NAA/ ^{23}Na ($t = 9.6$) was the most significant, followed by NAA/mIns ($t = 6.1$), and NAA/Cho ($t = 5.0$).

CONCLUSION: Although Glu concentration is reduced and mIns concentration is elevated in low-grade glioma tissue, the NAA/ ^{23}Na ratio was the most sensitive indicator of pathologic tissue.

Low-grade (WHO grade II) gliomas, including astrocytoma, oligodendroglioma, and mixed glioma (oligoastrocytoma), account for 10%–20% of primary brain tumors in adults.¹ Although such tumors are more indolent than high-grade gliomas, there is considerable variability in their clinical behavior.² They are capable of malignant transformation and, ultimately, are almost universally fatal. Pathologically, these tumors are diffuse and infiltrative but lack such anaplastic features as necrosis, endothelial proliferation, and mitotic activity.³

Tailoring treatment to the individual patient requires a better understanding of the factors that account for the variability in tumor behavior.^{4,5} Currently, neither the appearance of a low-grade glioma on conventional MR imaging nor tumor pathology can completely predict future tumor behavior or response to treatment. Metabolic profiling of these tumors with MR spectroscopy has the potential to improve our ability to predict the biological behavior and treatment response of

low-grade gliomas and to better delineate tumor boundaries. Previous in vitro and in vivo MR spectroscopy studies have identified metabolic markers that help noninvasively discriminate tumor type,^{6–8} aid in radiation treatment planning,⁹ or predict survival.¹⁰ Most studies have used long echotime spectroscopy acquisitions (TE ≥ 130 ms), limiting tumor metabolite characterization to the dominant peaks in the ^1H spectrum: *N*-acetylaspartate (NAA; a putative marker of neuronal viability), total creatine (Cr; involved in energy metabolism), choline-containing compounds (Cho; associated with membrane breakdown/synthesis), and lactate (associated with anaerobic glycolysis). Typically, low-grade glioma is characterized by reduced NAA due to reduced neuronal attenuation, reduced Cr due to a hypermetabolic state, and increased Cho, reflecting increased membrane turnover.^{6,8} The metabolites glutamate (Glu) and myo-inositol (mIns), measurable by shorter echotime ^1H -MR spectroscopy, may provide additional information about the pathologic state of the neoplasm. A previous study¹¹ has demonstrated that highly malignant tumors may release excess Glu to kill surrounding tissue and promote tumor growth, and increased Glu plus glutamine (Gln) has been measured previously in oligodendroglioma by ^1H -MR spectroscopy.¹² mIns activation of protein kinase C¹³ has also been associated with tumor malignancy. The limited use of short echotime ^1H -MR spectroscopy is due mainly to the difficulty in quantifying metabolites with complicated j-modulated spectral line shapes and the uncertainty introduced by less well-characterized macromolecule resonances beneath the metabolites of interest.

Tumors may also be characterized by the local concentration of total sodium, which is sensitive to changes in the tumor microstructure.^{14–16} For example, neoplastic cell proliferation

Received June 29, 2007; accepted after revision September 13.

From the Laboratory for Functional Magnetic Resonance Research (R.B.), Roberts Research Institute, London, Ontario, Canada; Department of Diagnostic Radiology and Nuclear Medicine (R.B.), Division of Neurosurgery, Department of Clinical Neurological Sciences and Department of Pathology, London Health Sciences Centre (J.F.M.), and Departments of Clinical Neurological Sciences and Oncology (C.J.W.), University of Western Ontario, London, Ontario, Canada.

This work was supported by the Roberts Research Institute, the Brain Tumour Foundation of Canada (grant No. R3399A02), the Plunkett Foundation, and the Canadian Institutes of Health Research (MME-15594).

Paper previously presented at: Annual Meeting of the International Society for Magnetic Resonance in Medicine; Abstract 668, May 7–13, 2005, Miami Beach, Fla.

Please address correspondence to Robert Bartha, Centre for Functional and Metabolic Mapping (CFMM), Roberts Research Institute, Box 5015, 100 Perth Dr, London, Ontario, N6A 5K8, Canada; e-mail: rob.bartha@imaging.roberts.ca

DOI 10.3174/ajnr.A0854

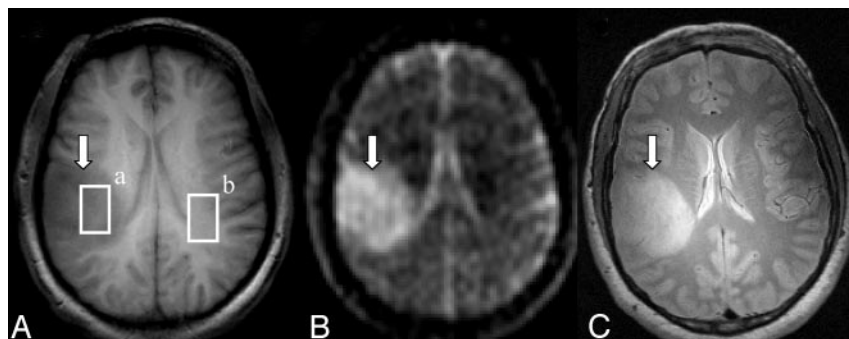


Fig 1. Transverse T1-weighted (A; T1/TR/TE = 500/9.5/5 ms), ^{23}Na (B; TR/TE = 25/3.8 ms), and FSE (C; TR/TE = 4500/15 ms) 4T MR images of a typical low-grade glioma in the same patient. The T1-weighted image has a 10-mm section thickness corresponding with the ^{23}Na image thickness. The white arrow identifies the low-grade glioma in each image. White boxes outline tissue regions in tumor (A) and on the contralateral side (B) studied by spectroscopy.

and packing, cell death, and necrosis expand the extracellular space in tumors. A defective blood-brain barrier in tumors also permits water, electrolytes, and proteins to enter the extracellular space leading to vasogenic edema. Because both intracellular and extracellular sodium levels may be increased in tumors, ^{23}Na MR imaging represents a potentially sensitive and noninvasive means of monitoring tissue sodium content related to cancer pathology.^{15–18}

The purpose of this study was to prospectively characterize the metabolic profile of low-grade gliomas by using ^1H -MR spectroscopy and to correlate metabolite levels with MR imaging-measured sodium signal intensity. Based on previous studies, it was hypothesized that levels of NAA would be reduced, and levels of Cho, mIns, Glu, and ^{23}Na signal intensity would be increased in low-grade glioma compared with normal tissue.

Methods

Thirteen patients with suspected low-grade glioma (7 male and 6 female; mean age, 44 ± 10 years) participated in this study, which was approved by the local ethics review board for health sciences research involving human subjects. Informed consent was obtained from all of the patients. Patients whose initial MR ($n = 12$) or CT ($n = 1$) imaging was considered highly suggestive of a diagnosis of low-grade glioma were considered eligible for the study. The treatment plan for each patient was not affected by the study and was determined by the treating oncologist. Pathologic classification of tumor type was obtained for patients when available from their clinical assessments. MR spectroscopy data from the parietal white matter of 10 young healthy control subjects who participated in a previous study¹⁹ were also retrospectively examined to provide context for the current study.

Data Acquisition

All of the in vivo images were acquired on a Varian (Palo Alto, Calif) whole body 4T MR scanner using a Sonata gradient coil (Siemens, Erlangen, Germany). Each study began with the acquisition of 3D inversion-prepared T1-weighted fast low-angle shot (FLASH) volumetric images (T1/TR/TE = 500/9.5/5 ms; 256×256 in-plane resolution; FOV, 24 cm; 64 sections; 2.5-mm thickness). In a subset of patients ($n = 10$), fast spin-echo (FSE) images (TR/TE = 4500–7000/15–123 ms; 256×256 in-plane resolution; FOV, 22–24 cm; 21 sections; 5-mm thickness) were also acquired to aid in positioning a single voxel within the tumor. Full spectra (metabolite and macromolecule, 128 averages), macromolecule spectra (128 averages), and water unsuppressed spectra (8 averages) were acquired as described previously¹⁹ from voxels with volumes ranging from 1.3 cm^3 to 17.9 cm^3 (average \pm SD = $6.9 \pm 4.6 \text{ cm}^3$) positioned within the tumor ($n = 13$) and in healthy tissue on the contralateral side ($n =$

10; Fig 1A). Spectra were localized by adiabatic selective refocusing (LASER²⁰; 500- μs dwell time; 2-kHz receiver bandwidth; TE, 46 ms; TR, 2.2 seconds) preceded by variable power RF pulses with optimized relaxation delays water suppression,²¹ using 3 pairs of 3.5-ms hyperbolic secant (HS2 and R15²⁰) adiabatic inversion pulses. Although an echo time of 46 ms is not normally considered a short echo time, the refocusing ability of the LASER pulse sequence due to the close spacing of adiabatic inversion pulses (6 ms) reduced j-coupling signal intensity modulation and allowed quantification of metabolites such as Glu²⁰ that are normally only quantified with shorter echo times (eg, 20 ms).

After anatomic imaging and ^1H -MR spectroscopy acquisitions, the ^1H hybrid birdcage coil was replaced with a 16-rung quadrature ^{23}Na hybrid birdcage coil without moving the subject. 3D single-quantum ^{23}Na volumetric images (64×64 in-plane resolution; FOV, 24 cm; 16 sections; 10-mm thickness; TR, 25 ms; bandwidth, 6.4 kHz; 24 averages; 10.2-minute acquisition time; TE, 3.8 ms) were acquired using a FLASH imaging sequence as described previously.^{22,23} A gradient-echo sequence with an asymmetric (67%) k -space readout (43 of 64 points) was chosen instead of a spin-echo sequence to minimize echo time and energy deposition and to increase signal-to-noise ratio (SNR).²² At the minimum echo time achieved (3.8 ms), this pulse sequence was primarily sensitive to the long T2 component of the ^{23}Na signal intensity. To provide greater sensitivity to the short T2 component, sequences capable of shorter echo times must be used.^{24,25} Excitation power levels were calibrated for each acquisition to maximize SNR (Ernst angle, $\sim 49^\circ$, assuming that T1 of ^{23}Na is 60 ms at 4T). The ^{23}Na images were acquired at the same positions and with the same FOV as the ^1H FLASH images (1 ^{23}Na image = 4 ^1H images) and, therefore, did not require further alignment or registration.

Data Processing and Metabolite Quantification

All of the spectroscopy data were line-shape corrected,²⁶ processed (the macromolecule contribution removed and residual water subtracted), and metabolites quantified by a single researcher as described previously.¹⁹ To quantify metabolite levels, metabolite spectra were fit in the time domain by using a Levenberg-Marquardt minimization routine incorporating prior knowledge from 19 metabolite line shapes.²⁷ Metabolite levels were normalized to the level of unsuppressed water within the tissue of each voxel.²⁸ To estimate the concentration of unsuppressed water in each voxel, the water content was estimated at 81%, 71%, and 94% in gray matter, white matter, and low-grade tumor, respectively.^{7,28} The average ratio of gray matter/white matter/CSF was determined for each voxel by segmenting the T1-weighted images into gray matter/white matter/CSF probability maps using Statistical Parametric Mapping (SPM5,²⁹) in Matlab (Macintosh v7.3.0.298; The Mathworks, Natick, Mass). To perform

Relaxation time constants used in metabolite quantification

Variable	T1 Time Constant, ms	T2 Time Constant, ms	Reference
Gray matter–water	1361	93	30, 31
White matter–water	814	102	30, 31
Low-grade glioma–water	814	175	6, 31
NAA	1630	401	32, 33
Cr	1720	273	32, 33
Cho	1290	330	32, 33
Other metabolites	1550	335	19

Note:—NAA indicates *N*-acetylaspartate; Cr, creatine; Cho, choline.

the analysis, the T1-weighted images were warped to a standard space, and a template of tissue probability was used. The contribution of gray matter, white matter, and CSF to each voxel in normal tissue was calculated by using a plug-in written in ImageJ (National Institutes of Health, Bethesda, Md). Because the same method could not be used to determine the contribution of glioma tissue to a voxel, an average ratio of glioma tissue/CSF within a voxel was estimated as 98%/2% in low-grade tumors. A correction was made for T1 and T2 relaxation signal intensity loss in water and metabolite spectra by using estimates of these time constants from the literature^{6,19,30–33} (Table). For spectra acquired in tissue contralateral to the tumor, a weighted average of relaxation time constants based on the average gray matter/white matter tissue fraction was used to determine T1 and T2 signal intensity attenuation. The measurement of metabolite T2 values in tumors has been only sparsely reported, with considerable variability for NAA, Cr, and Cho.^{6,34–36} Due to the inconsistency in these reports, the values for normal white matter were used in the current study. The average line width (full width at half maximum) of the unsuppressed water spectra was quantified for tumors and control data to support the use of a greater T2 time constant in glioma tissue.⁶ Metabolite levels were calculated by using equations 1 and 2 in Stanley et al,²⁸ but also incorporating the relaxation time corrections detailed above, as follows:

$$1) \quad A_{met} = Area_{metabolite} \times R_{Metabolite}$$

$$2) \quad A_{H_2O} = Area_{water} \times [(F_{Gray} \cdot R_{Gray}) + (F_{White} \cdot R_{White}) + (F_{Glioma} \cdot R_{Glioma})]$$

where A_{met} and A_{H_2O} are defined in reference 28, $Area_{metabolite}$ is the fitted area of a metabolite, $Area_{water}$ is the fitted area of the water peak in the water unsuppressed spectrum, F is the fraction of specified tissue in the voxel (gray matter, white matter, or glioma), and R is the relaxation correction factor for a specified tissue and metabolite in equations 1 and 2 defined as follows:

$$3) \quad R_{Tissue/Metabolite} = [(1 - e^{-TR/T1}) \times e^{-TE/T2}]^{-1}$$

where $T1$ and $T2$ are the relaxation time constants defined in the Table corresponding with the tissue or metabolite, and TR is the repetition time and TE is the echo time of the spectroscopy sequence. An extra term ($0.937 \cdot f_{glioma}$) was also added to equation 2 in Stanley et al²⁸ to correct for the increased water concentration in glioma tissue (where f_{glioma} is the fraction of glioma tissue in the voxel).

Sodium images were reconstructed using a 3D fast Fourier transform without zero-filling or spatial filters. The average sodium signal intensities for pixels in the sodium image that contributed to each spectroscopy voxel (including all of the sections that intersected with the voxel) were automatically calculated using a plug-in written for

ImageJ. Pixels on the boundary of the voxel were weighted by the fraction of the pixel in the sodium image that was contained within the spectroscopy voxel. The sodium signal intensity acquired at 3.8-ms echo time is dominated by the long T2* relaxation component.²² The T2* of this component (18 ms) has been characterized previously in normal tissue²² and was measured in 1 low-grade glioma patient in the current study (27 ms) to estimate T2* in low-grade glioma. Therefore, the average sodium intensities in voxels within glioma were corrected for the long component of T2* relaxation by using a T2* time constant of 27 ms. The corrected sodium intensity was then normalized to the corrected ²³Na signal intensity (by using a T2* time constant of 18 ms) from a region of normal-appearing white matter (manually outlined) on the contralateral side. Therefore, reported values represent the percentage of sodium signal intensity normalized to white matter.

Statistical Analysis

All of the statistical tests were performed in Prism (v4.0b for Macintosh, 2004; GraphPad Software, San Diego, Calif). The line widths of the unsuppressed water spectra from tumor and contralateral tissue were compared using a 2-sided Student *t* test ($P < .05$ was considered statistically significant). The average (\pm SD) level of all 19 metabolites and ²³Na signal intensity was determined in healthy tissue and in tumor tissue. Average metabolite levels measured with coefficients of variation (SD/mean \times 100%) of less than 50% in control tissue (NAA, Glu, Cr, Cho, and mIns) were compared. To determine whether metabolite levels and tissue ²³Na were different in low-grade glioma and normal tissue, levels from a low-grade tumor were compared with levels from contralateral tissue in the same subjects. These comparisons were made with 2-sided Student *t* test ($P < .05$ was considered statistically significant). To determine whether levels of NAA and ²³Na signal intensity were correlated with other measured metabolite levels that were found to be significantly different between groups, the Pearson correlation coefficients and associated *P* values were calculated. Metabolites were considered significantly correlated if r^2 was >0.25 and *P* value was $<.05$.

Based on the absolute metabolite level changes hypothesized, several metabolite ratios (NAA/mIns, NAA/²³Na, and NAA/Cho) were also examined to determine whether these would provide greater discrimination between glioma tissue and normal tissue. Average ratios were compared between tissues by using a 2-sided Student *t* test ($P < .05$ was considered to indicate a statistically significant difference).

Results

Pathologic Classification

Of the 13 study subjects, 3 underwent gross total resection, 3 underwent subtotal resection, and 5 underwent biopsy. The remaining 2 patients continue to be managed expectantly based on clinical and radiologic stability and have not yet had a tissue diagnosis made. Among those with a tissue diagnosis, there were 5 grade 2 oligodendrogliomas, 4 tumors where pathology confirmed grade 2 glioma but could not specify histologic subtype (2 of these were labeled “probable oligodendroglioma”), and 2 anaplastic astrocytomas. These 2 patients were excluded from further analysis. It should be noted that 1 of these patients was enrolled after CT. This patient went on to have a contrast-enhanced MR imaging subsequent to being entered in the study, which demonstrated a small area of con-

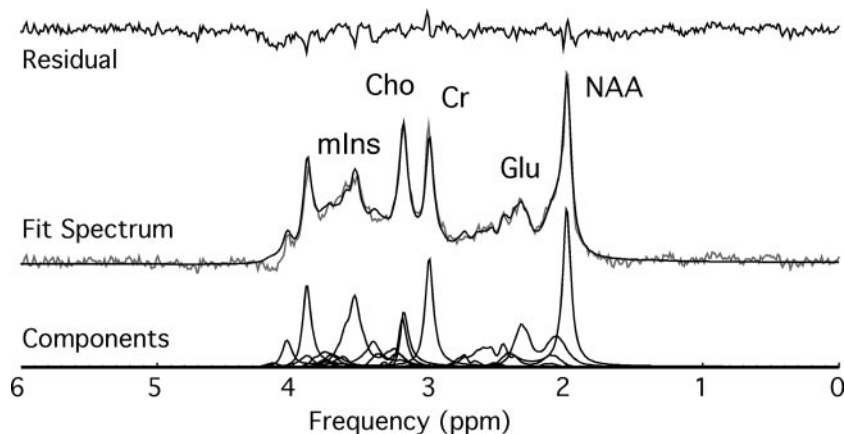


Fig 2. White matter MR spectrum (center gray line) with fit (center black line) superimposed. Individual metabolite components are shown beneath, along with the fit residual (top).

oma (Fig 3) highlight the variations in detected metabolite levels between patients and compared with levels in normal tissue (Fig 2), particularly for NAA, Glu, Cho, and mIns. Unsuppressed water spectra from the low-grade tumors had a narrower line width (5.8 ± 2.8 Hz) than spectra from normal tissue on the contralateral side (9.3 ± 2.5 Hz; $P < .01$).

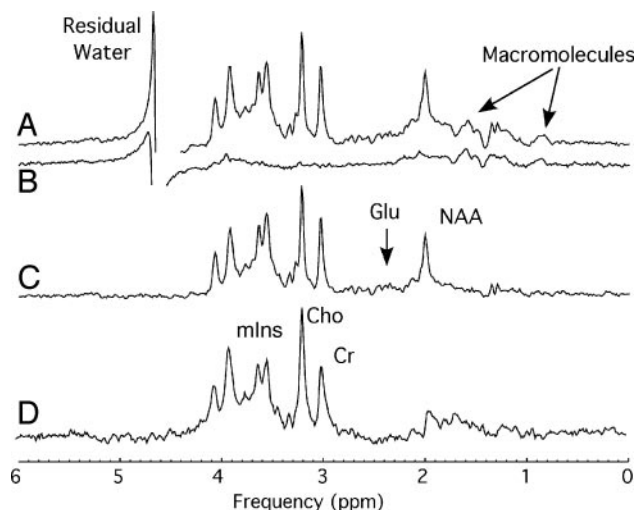


Fig 3. A, A representative LASER (TR/TE = 2200/46 ms) spectrum (including metabolite and macromolecule components) from 1 patient with low-grade glioma. The corresponding metabolite nulled macromolecule spectrum (B) is subtracted from a fully processed spectrum (A). C, The resultant spectrum after water removal demonstrates the efficacy of the macromolecule removal. D, A second dataset acquired in a different subject is also provided. Spectra have been line broadened by a 2-Hz Lorentzian filter for display.

trast enhancement within the tumor that was not appreciated on CT imaging.

Imaging and Spectroscopy

T1-weighted and FSE anatomic images (Fig 1) were used to position the voxel for ^1H -MR spectroscopy. The low-grade glioma is clearly visible in the T1-weighted, T2*-weighted ^{23}Na , and FSE images (white arrow, Fig 1). The location of the 2 spectroscopy voxels acquired in 1 subject are shown (Fig 1) corresponding with locations within the tumor (voxel a) and on the contralateral side (voxel b). The average ratio of gray matter/white matter/CSF was 38%/56%/6% in the voxels positioned on the contralateral side. This ratio varied from voxel to voxel; in particular, the CSF contribution ranged from 1% to 9% in the voxel studies. A typical spectrum acquired from normal white matter in a control subject without cancer (Fig 2) demonstrates the expected relative amplitudes of each metabolite. The fit result, with the residual shown above and the individual metabolite components shown below (Fig 2), demonstrates the appropriateness of the metabolite components included in the spectral fitting. Representative spectra from within the tumors of 2 different patients with low-grade gli-

Metabolite Levels and ^{23}Na Signal Intensity

The average levels of several metabolites and relative ^{23}Na signal intensity were different in low-grade tumors ($n = 11$) compared with contralateral control tissue ($n = 10$) in the same patients (Fig 4). Metabolite levels from white matter in a separate group of healthy control subjects¹⁹ also had less variability than the measures made from the contralateral tissue (Fig 4) sampled in patients (which contained a mixture of gray and white matter). Significant average decreases were observed for NAA (69%; $P < .001$) and Glu (61%; $P = .004$), and average increases were observed for mIns (90%; $P = .003$), Cho (52%; $P = .025$), and sodium signal intensity (102%; $P < .001$) in low-grade glioma tissue compared with tissue on the contralateral side in the same patients. Had a Bonferroni correction been applied, these differences would have remained significant except for the increase in Cho. Combining data from the low-grade glioma and contralateral control tissue, significant correlations were observed between NAA and Glu ($r^2 = 0.27$; slope = 0.5 ± 0.2 ; y intercept = 2.3 ± 1.5 ; $P < .05$) and NAA and mIns ($r^2 = 0.32$; slope = -0.7 ± 0.2 ; y intercept = 16.1 ± 1.9 ; $P < .01$; Fig 5). Significant correlations were also observed between ^{23}Na signal intensity and NAA ($r^2 = 0.34$; slope = -0.04 ± 0.01 ; y intercept = 13.5 ± 2.2 ; $P < .01$) and ^{23}Na signal intensity and Glu ($r^2 = 0.35$; slope = -0.04 ± 0.01 ; y intercept = 11.1 ± 1.9 ; $P < .01$; Fig 5).

Follow-up comparisons were made between contralateral control and grade 2 glioma for ratios of NAA/mIns, NAA/ ^{23}Na , and NAA/Cho (Fig 6). The NAA/Cho ratio is often considered an indicator of tumor malignancy. All 3 of the ratios were lower ($P < .001$) in glioma tissue compared with contralateral control; however, based on the t statistic, NAA/ ^{23}Na ($t = 9.6$) was the most significant, followed by NAA/mIns ($t = 6.1$) and NAA/Cho ($t = 5.0$). These differences would also have remained significant had a Bonferroni correction been applied.

Discussion

Human low-grade glioma was studied in vivo at 4T in 11 patients by using ^1H -MR spectroscopy (incorporating the direct measurement of macromolecules in the spectrum) and ^{23}Na imaging. The results showed that absolute levels of Glu and NAA were significantly decreased, whereas levels of mIns and ^{23}Na signal intensity were significantly increased in low-grade glioma tissue. Pooling all of the data, a significant positive correlation was observed between NAA and Glu, whereas a

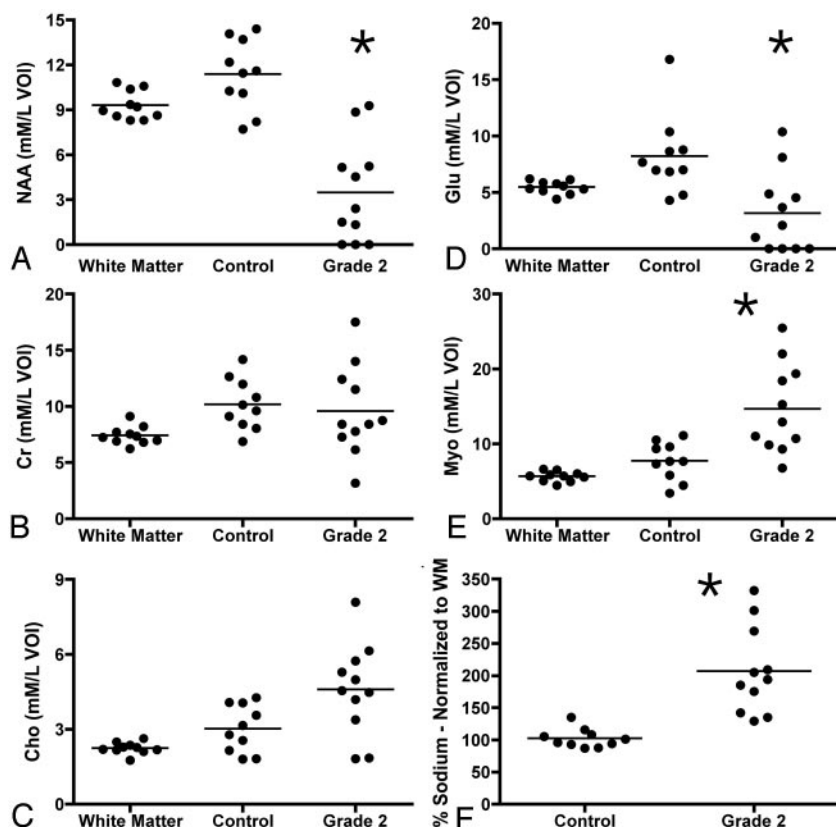


Fig 4. Scatter plot of individual metabolite levels (millimoles per liter of VOI) for NAA (A), Cr (B), Cho (C), Glu (D), mIns (E), and percentage of sodium signal intensity (F) in grade II glioma and on the contralateral side are shown along with horizontal lines indicating the metabolite averages. Data from a reference region of homogeneous white matter are also included from a previous study.¹⁹ The sodium signal intensity in arbitrary units is reported for grade 2 glioma and from the contralateral side. Asterisks indicate significant differences between grade 2 glioma and control (NAA, Glu, mIns, and sodium).

significant negative correlation was observed between NAA and mIns and between ^{23}Na signal intensity and both NAA and Glu. To our knowledge, this is the first study to measure levels of ^{23}Na and ^1H metabolites in the same tumor and to show that ^{23}Na levels correlate with tissue metabolite levels. The analysis indicates that the ratio of NAA/ ^{23}Na may be a more sensitive indicator of tissue pathology than the use of metabolite levels alone.

Because gliomas represent a proliferation of glial-type cells, the density of neurons within these tumors is lower than normal tissue. The observation of decreased NAA levels is consis-

tent with previous studies^{6-8,12} and with the notion that NAA is predominantly localized within neurons.³⁷ The observed decrease in Glu contradicts one previous study¹² performed at 1.5T that suggested that increased Glu + Gln may be characteristic of low-grade gliomas. The discrepancy may be due to the removal of the macromolecule baseline signal intensity in the current study before quantification. Because the macromolecule resonances overlap with NAA and, to some extent both Glu and Gln resonances between 2.0 and 2.5 ppm, failure to account for these signals may lead to the overestimation of other metabolites of interest. A careful examination of the macromolecule spectra acquired in the current study indicates that the inversion times used for metabolite nulling were effective in tumor tissue, as well as normal tissue. The observed increase in mIns is consistent with previous studies.^{8,13} The correlation of NAA with Glu and mIns lends further support to the idea that levels of these metabolites are different in neurons and glioma cells. When the level of NAA approached 0 (implying that no neurons were present in the sample) there was very little extrapolated Glu (2.3 mmol/L/L volume of interest [VOI]) and very high extrapolated mIns (16.2 mmol/L/L VOI). Increased Cho was also detected in low-grade glioma as expected.^{6,8} Although decreased Cr⁸ has been reported

previously compared with normal-appearing white matter, a significant difference in Cr was not detected in this cohort.

The increased sodium signal intensity observed in the current study is also consistent with previous reports^{14,15,18} and probably indicates expansion of the extracellular space and increased intracellular sodium concentration. ^{23}Na signal intensity was inversely correlated with both NAA and Glu as expected. In both cases, extrapolation to NAA and Glu levels of 0 produced levels of ^{23}Na that were roughly 3 times higher than those observed in normal white matter. As a follow-up test, metabolite ratios were computed for

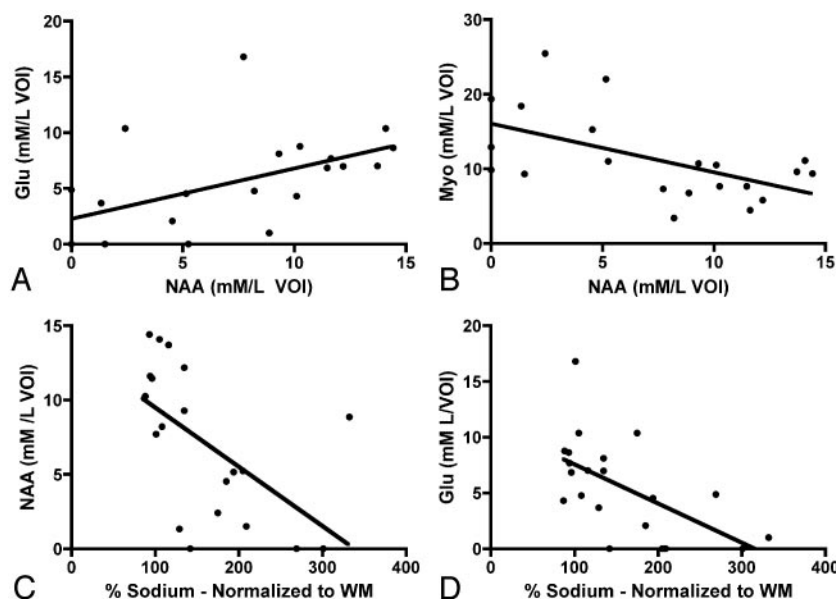


Fig 5. Correlation of pooled NAA with Glu (A) and mIns (B) and of percentage of sodium signal intensity normalized to white matter (WM) with NAA (C) and Glu (D). Linear regression lines are superimposed. Details of the correlation results are described in the text.

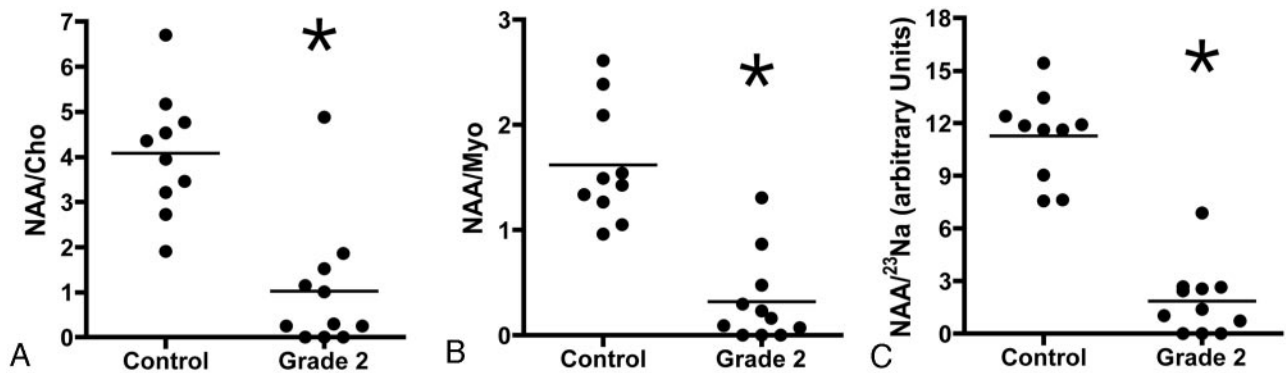


Fig 6. Metabolite ratios for NAA/Cho (A), NAA/mIns (B), and NAA/²³Na (C). Asterisks represent significantly lower value compared with control.

NAA/Cho (commonly reported as decreased in tumors) and for NAA/mIns and NAA/²³Na to determine whether these ratios may represent more sensitive biomarkers of tumor tissue. Although all 3 of the indicators were highly sensitive, the NAA/²³Na ratio was the most significant, demonstrating the least variability and, therefore, greatest separation between groups.

There are several limitations to this study. The sample size in this pilot study was small and did not allow for comparison of metabolite levels in different tumor types. However, this pilot study indicates that a larger study of the use of the NAA/²³Na ratio to evaluate tumor extent and grade may be warranted. Several methodologic issues must also be discussed. In the acquisition of spectroscopy data, a voxel size was chosen based on the size of individual tumors; specifically, voxels were made as large as possible to increase the SNR associated with spectroscopy measures while placing the voxel edges within the tumor boundary as visualized on T1- and T2-weighted images. Signal intensity-to-noise ratio is an important consideration, particularly for the quantification of metabolites such as Glu and mIns.³⁸ The same voxel dimensions were used in contralateral tissue and, therefore, incorporated gray matter, white matter, and CSF. Although the partial volume of these tissue components was determined for each voxel and incorporated in the final metabolite level calculations, greater variability in control data acquired in this study was observed compared with data from a previous study of homogeneous parietal lobe white matter.¹⁹ This variability is probably due to differences in metabolite levels in different parts of the brain and different signal intensity-to-noise ratios between spectra and does not represent abnormalities in uninvolved brain regions.

Absolute quantification of tumor metabolite levels is critical for accurate characterization of tumor types to aid in non-invasive diagnosis.³⁹ The careful measurement by inversion nulling and removal of the macromolecule baseline¹⁹ before metabolite quantification increased the accuracy of metabolite level measurements, particularly in tumor spectra, where macromolecule and lipid signal intensity are known to fluctuate. In the quantification of metabolites, estimates were made for the T1 and T2 time constants within the tissue, because it is not possible to measure all such parameters in each subject. The use of a longer T2 for water in tumor⁴⁰ was supported by the narrower line widths (38% decrease) of the water-suppressed spectra from tumors in the current study. The overall impact of the relaxation times used for tumor tissue was to

increase metabolite estimates by approximately 30% compared with what they would have been had the same relaxation times been used as for normal tissue. A greater water concentration was also used to estimate metabolite levels in low-grade glioma, resulting in higher metabolite values (~25%) than if the concentration for normal tissue had been used. Although there is some uncertainty regarding the estimates of relaxation times and water content, failure to make these adjustments would lead to the underestimation of metabolite concentration. Had these adjustments not been made, a greater difference in NAA and Glu would have been reported, whereas the observed difference in mIns would have decreased. However, the quantified metabolite levels are consistent with the changes observed visually in tumor spectra (Fig 3). The use of metabolite ratios also removes these biases and, therefore, may also represent reliable biomarkers of tumor physiology. With regard to the sodium imaging, a longer T2* (27 ms) was used to correct ²³Na signal intensity in tumor tissue compared with control tissue (18 ms), consistent with a previous study.¹⁴ If the same T2* had been used to correct ²³Na signal intensity in tumor and contralateral tissue, a greater signal intensity difference would have been observed between these tissue types. Therefore, future studies with longer ²³Na imaging echo time may provide even greater contrast; however, this increase in contrast must be weighted against the loss in signal intensity-to-noise ratio at longer echo times, particularly for ²³Na, which has very short transverse relaxation times. In the current study, it is estimated that only 49% of the sodium signal intensity was sampled at the 3.8-ms echo time used.

Conclusion

Low-grade glioma was characterized with low levels of NAA and Glu, high levels of mIns, and high levels of ²³Na, whereas the ratio of NAA/²³Na most clearly differentiated glioma tissue from normal tissue. Future work should examine the potential for these metabolic parameters to distinguish low-grade gliomas destined for indolent behavior from those destined for early malignant transformation to identify those tumors most likely to benefit from specific treatment interventions or to delineate tumor boundaries (identify infiltration).

References

- Macdonald DR. Low-grade gliomas, mixed gliomas, and oligodendrogliomas. *Semin Oncol* 1994;21:236–48

2. Cavaliere R, Lopes MB, Schiff D. **Low-grade gliomas: an update on pathology and therapy.** *Lancet Neurol* 2005;4:760–70
3. Perry A. **Pathology of low-grade gliomas: an update of emerging concepts.** *Neuro-oncol* 2003;5:168–78
4. Pignatti F, van den Bent M, Curran D, et al. **Prognostic factors for survival in adult patients with cerebral low-grade glioma.** *J Clin Oncol* 2002;20:2076–84
5. Stege EM, Kros JM, de Bruin HG, et al. **Successful treatment of low-grade oligodendroglial tumors with a chemotherapy regimen of procarbazine, lomustine, and vincristine.** *Cancer* 2005;103:802–09
6. Isobe T, Matsumura A, Anno I, et al. **Quantification of cerebral metabolites in glioma patients with proton MR spectroscopy using T2 relaxation time correction.** *Magn Reson Imaging* 2002;20:343–49
7. Tong Z, Yamaki T, Harada K, et al. **In vivo quantification of the metabolites in normal brain and brain tumors by proton MR spectroscopy using water as an internal standard.** *Magn Reson Imaging* 2004;22:1017–24
8. Howe FA, Barton SJ, Cudlip SA, et al. **Metabolic profiles of human brain tumors using quantitative in vivo 1H magnetic resonance spectroscopy.** *Magn Reson Med* 2003;49:223–32
9. Nelson SJ, Graves E, Pirzkall A, et al. **In vivo molecular imaging for planning radiation therapy of gliomas: an application of 1H MRSI.** *J Magn Reson Imaging* 2002;16:464–76
10. Li X, Jin H, Lu Y, et al. **Identification of MRI and 1H MRSI parameters that may predict survival for patients with malignant gliomas.** *NMR Biomed* 2004;17:10–20
11. Takano T, Lin JH, Arcuino G, et al. **Glutamate release promotes growth of malignant gliomas.** *Nat Med* 2001;7:1010–15
12. Rijpkema M, Schuurin J, van der Meulen Y, et al. **Characterization of oligodendrogliomas using short echo time 1H MR spectroscopic imaging.** *NMR Biomed* 2003;16:12–18
13. Castillo M, Smith JK, Kwok L. **Correlation of myo-inositol levels and grading of cerebral astrocytomas.** *AJNR Am J Neuroradiol* 2000;21:1645–49
14. Turski PA, Houston LW, Perman WH, et al. **Experimental and human brain neoplasms: detection with in vivo sodium MR imaging.** *Radiology* 1987;163:245–49
15. Ouwerkerk R, Bleich KB, Gillen JS, et al. **Tissue sodium concentration in human brain tumors as measured with 23Na MR imaging.** *Radiology* 2003;227:529–37
16. Schepkin VD, Ross BD, Chenevert TL, et al. **Sodium magnetic resonance imaging of chemotherapeutic response in a rat glioma.** *Magn Reson Med* 2004;53:85–92
17. Winkler SS. **Sodium-23 magnetic resonance brain imaging.** *Neuroradiology* 1990;32:416–20
18. Thulborn KR, Davis D, Adams H, et al. **Quantitative tissue sodium concentration mapping of the growth of focal cerebral tumors with sodium magnetic resonance imaging.** *Magn Reson Med* 1999;41:351–59
19. Kassem MN, Bartha R. **Quantitative proton short-echo-time LASER spectroscopy of normal human white matter and hippocampus at 4 Tesla incorporating macromolecule subtraction.** *Magn Reson Med* 2003;49:918–27
20. Garwood M, DelaBarre L. **The return of the frequency sweep: designing adiabatic pulses for contemporary NMR.** *J Magn Reson* 2001;153:155–77
21. Tkac I, Starcuk Z, Choi IY, et al. **In vivo 1H NMR spectroscopy of rat brain at 1 ms echo time.** *Magn Reson Med* 1999;41:649–56
22. Bartha R, Menon RS. **Long component time constant of 23Na T*2 relaxation in healthy human brain.** *Magn Reson Med* 2004;52:407–10
23. Parrish TB, Fieno DS, Fitzgerald SW, et al. **Theoretical basis for sodium and potassium MRI of the human heart at 1.5 T.** *Magn Reson Med* 1997;38:653–61
24. Boada FE, Shen GX, Chang SY, et al. **Spectrally weighted twisted projection imaging: reducing T2 signal attenuation effects in fast three-dimensional sodium imaging.** *Magn Reson Med* 1997;38:1022–28
25. Boada FE, Gillen JS, Shen GX, et al. **Fast three dimensional sodium imaging.** *Magn Reson Med* 1997;37:706–15
26. Bartha R, Drost DJ, Menon RS, et al. **Spectroscopic lineshape correction by QUECC: combined QUALITY deconvolution and eddy current correction.** *Magn Reson Med* 2000;44:641–45
27. Bartha R, Drost DJ, Williamson PC. **Factors affecting the quantification of short echo in-vivo 1H MR spectra: prior knowledge, peak elimination, and filtering.** *NMR Biomed* 1999;12:205–16
28. Stanley JA, Drost DJ, Williamson PC, et al. **The use of a priori knowledge to quantify short echo in vivo 1H MR spectra.** *Magn Reson Med* 1995;34:17–24
29. Ashburner J, Friston K. **Multimodal image coregistration and partitioning—a unified framework.** *Neuroimage* 1997;6:209–17
30. Bartha R, Michaeli S, Merkle H, et al. **In vivo 1H2O T2+ measurement in the human occipital lobe at 4T and 7T by Carr-Purcell MRI: detection of microscopic susceptibility contrast.** *Magn Reson Med* 2002;47:742–50
31. Mason GF, Chu WJ, Hetherington HP. **A general approach to error estimation and optimized experiment design, applied to multislice imaging of T1 in human brain at 4.1 T.** *J Magn Reson* 1997;126:18–29
32. Posse S, Cuenod CA, Risinger R, et al. **Anomalous transverse relaxation in 1H spectroscopy in human brain at 4 Tesla.** *Magn Reson Med* 1995;33:246–52
33. Michaeli S, Garwood M, Zhu XH, et al. **Proton T2 relaxation study of water, N-acetylaspartate, and creatine in human brain using Hahn and Carr-Purcell spin echoes at 4T and 7T.** *Magn Reson Med* 2002;47:629–33
34. Usenius JP, Vainio P, Hernesniemi J, et al. **Choline-containing compounds in human astrocytomas studied by 1H NMR spectroscopy in vivo and in vitro.** *J Neurochem* 1994;63:1538–43
35. Matsumura A, Isobe T, Anno I, et al. **Correlation between choline and MIB-1 index in human gliomas. A quantitative in proton MR spectroscopy study.** *J Clin Neurosci* 2005;12:416–20
36. Manton DJ, Lowry M, Blackband SJ, et al. **Determination of proton metabolite concentrations and relaxation parameters in normal human brain and intracranial tumours.** *NMR Biomed* 1995;8:104–12
37. Block W, Traber F, Flacke S, et al. **In-vivo proton MR-spectroscopy of the human brain: assessment of N-acetylaspartate (NAA) reduction as a marker for neurodegeneration.** *Amino Acids* 2002;23:317–23
38. Bartha R. **Effect of signal-to-noise ratio and spectral linewidth on metabolite quantification at 4 T.** *NMR Biomed* 2007;20:512–21
39. Law M, Yang S, Wang H, et al. **Glioma grading: sensitivity, specificity, and predictive values of perfusion MR imaging and proton MR spectroscopic imaging compared with conventional MR imaging.** *AJNR Am J Neuroradiol* 2003;24:1989–98
40. Whittall KP, MacKay AL, Graeb DA, et al. **In vivo measurement of T2 distributions and water contents in normal human brain.** *Magn Reson Med* 1997;37:34–43